



Calhoun: The NPS Institutional Archive

Faculty and Researcher Publications

Faculty and Researcher Publications Collection

2014

High strain-rate response of spiropyran mechanophores in PMMA

Hemmer, J.R.

J. R. Hemmer, P. D. Smith, M. van Horn, S. Alnemrat, B. P. Mason, J. Read de Alaniz, S. Osswald, and J. P. Hooper. "High strain-rate response of spiropyran mechanophores in PMMA. "J. Polym. Sci. B: Polym. Phys. 52, 1347 (2014).



Calhoun is a project of the Dudley Knox Library at NPS, furthering the precepts and goals of open government and government transparency. All information contained herein has been approved for release by the NPS Public Affairs Officer.

Dudley Knox Library / Naval Postgraduate School
411 Dyer Road / 1 University Circle
Monterey, California USA 93943

<http://www.nps.edu/library>

High Strain-Rate Response of Spiropyran Mechanophores in PMMA

James R. Hemmer,¹ Patrick D. Smith,² Matt van Horn,² Sufian Alnemrat,² Brian P. Mason,³ Javier Read de Alaniz,¹ Sebastian Osswald,² Joseph P. Hooper²

¹Department of Chemistry and Biochemistry, University of California, Santa Barbara, California 93106

²Department of Physics, Naval Postgraduate School, 833 Dyer Way, Monterey, California 93943

³Research Department, Naval Surface Warfare Center, Indian Head Division, 3767 Strauss Ave., Indian Head, Maryland 20640

Correspondence to: J. P. Hooper (E-mail: jphooper@nps.edu)

Received 21 June 2014; accepted 24 July 2014; published online 18 August 2014

DOI: 10.1002/polb.23569

ABSTRACT: We report the high strain-rate response of a spiropyran (SP) mechanophore in poly(methylmethacrylate). Previous work on this system has demonstrated a reversible bond scission in the SP under local tensile force, converting it to a fluorescent merocyanine form. A Hopkinson bar was used to apply fast compressive loads at rates from 10^2 to 10^4 s⁻¹, resulting in significant activation of the SP near fracture surfaces. However, comparison with a similar thermochromic SP reveals that much of the observed activation likely arises from thermal effects during high-rate fracture. These results show the importance of a thermally active control system in distin-

guishing mechanochromic response during high-rate loading. Microscale fluorescence mapping of the fracture surfaces using a confocal Raman microspectrometer suggests that some distinct mechanical activation may be occurring in craze-like regions during fibril rupture. The thermal response of the SP is useful in its own right for characterizing plastic heating regions during dynamic fracture. Published 2014.† J. Polym. Sci., Part B: Polym. Phys. **2014**, 52, 1347–1356

KEYWORDS: compression; dyes/pigments; failure; fluorescence; impact resistance; mechanical properties; sensors

INTRODUCTION Mechanochemistry, the use of mechanical force to break chemical bonds, has recently garnered considerable attention in both the chemistry and the polymer communities.^{1–3} Solution-based mechanochemistry incorporates a mechanophore at the center of a long polymer chain that is subjected to mechanical force via cavitation from an ultrasonic horn. This method of applying force has proven capable of breaking chemical bonds from a range of structures, including triazoles,⁴ Diels–Alder adducts,⁵ cyclopropanes,⁶ and cyclobutanes.⁷ In the solid, polymer-bound mechanophores have been activated through stretching,⁸ squeezing,^{9,10} and even mastication.¹¹

Polymer mechanochemistry holds exciting opportunities for analyzing chain dynamics and bulk mechanical response with a very high degree of spatial resolution.^{12–15} For stress sensing applications, the majority of work has focused on spiropyran (SP) based sensors, which can be attached directly into a linear polymer chain^{8,13–20} or function as cross-linking groups.^{16,21} Under slow, quasi-static tensile stress this optically yellow functional group undergoes a reversible C–O bond scission to a merocyanine (MC) form that is red [see Fig. 1(a)]. Visible light

reconverts the merocyanine back to the uncolored SP form.

Localized temperature can also induce the transformation to merocyanine, but this varies with the polymer matrix and means of mechanophore integration. Temperatures above approximately 50 °C activate SP in linear poly(methylacrylate) (PMA),⁸ but SP in linear PMMA is thermally inactive at 90 °C.¹³ This is a particularly important point for the high strain-rate loading conditions discussed here, as plastic deformation during fast loading will lead to temperature increases not observed in standard quasistatic mechanical tests. In the majority of reported tests on SP mechanophores, large plastic strain and significant chain mobility were necessary to achieve mechanical activation.¹³ Recent work by Grady and coauthors reported activation of SP in polystyrene following laser shock on a thin film of material, demonstrating that the SP can respond on fast timescales and at high loading rates.²² This suggested the possibility of high-rate activation at much lower strains than seen in previous work. A difunctional control, with the polymer attached so as not to provide tension across the mechanically active bond in the SP, was also tested in this work and showed minimal fluorescence. This difunctional control is UV-active, but

Additional Supporting Information may be found in the online version of this article.

Published 2014. †This article is a U.S. Government work and is in the public domain in the USA.

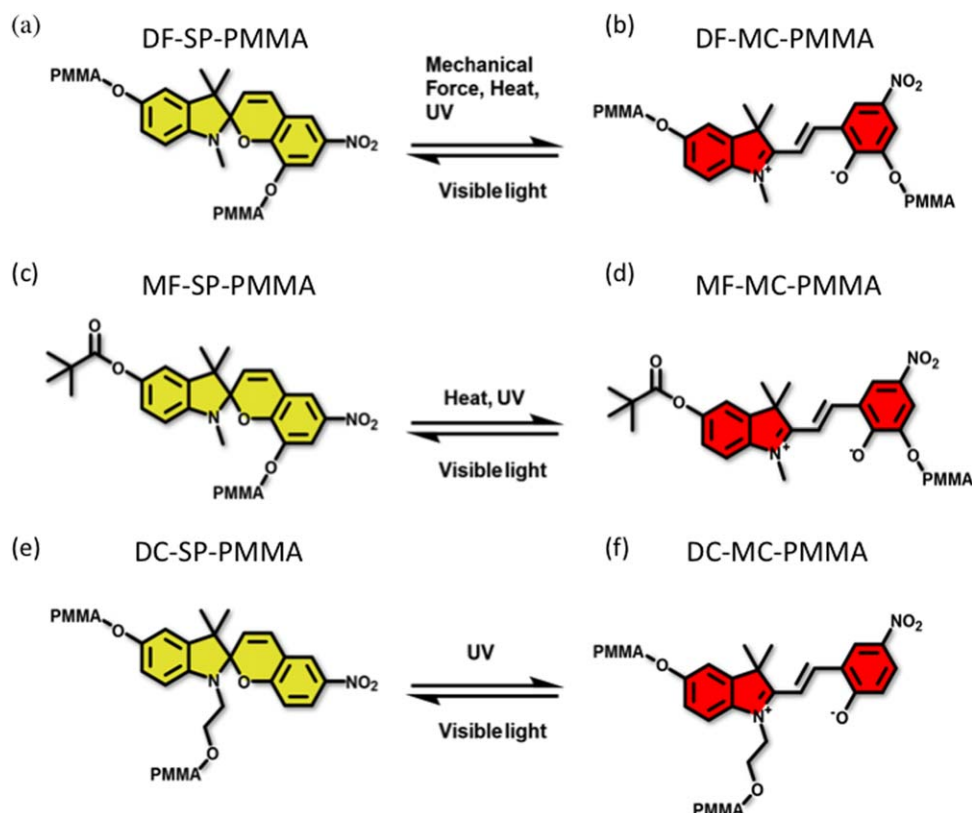


FIGURE 1 Chromophores tested in this study. [Color figure can be viewed in the online issue, which is available at wileyonlinelibrary.com.]

thermally and mechanically inert. It is desirable to further explore the mechanochemical response of the SP under fast loading, and determine if the mechanical activation can be fully distinguished from thermal effects that occur in these loading regimes. As chain and bulk polymer dynamics depend very sensitively on the strain-rate of the loading, a mechanophore that can activate on microsecond timescales and respond purely to localized force might serve as an interesting probe of dynamic fracture and mechanical response.

Herein, we report the high-rate response of mechanochromic and thermochromic poly(methylmethacrylate) (PMMA) that incorporates a SP sensor molecule. The SP was incorporated both as a pendant on PMMA chains (thermally responsive configuration) and as a crosslinking group between chains (mechanically and thermally responsive configuration). A split Hopkinson pressure bar was used to provide controlled high strain-rate loading on samples, and fluorescence was quantified by confocal Raman microspectrometry on recovered samples. Significant activation of the mechanophore is observed in all samples, primarily at fracture surfaces. However, the similarity of response between the mechanochromic and thermochromic configurations suggests that the majority of this activation is due to heating effects from the plastic dissipation zone of cracks, and not from mechanochemistry alone. A difunctional control similar to that tested in previous work shows no response under intense high-rate load-

ing. These results show the importance of a thermal control system for distinguish mechanochromic response under rapid stress loading, an issue that does not occur for standard low-rate mechanical tests. Mesoscale scans of the SP fluorescence on recovered fragments do suggest some distinct mechanical activation may be occurring, primarily in craze-like regions. The thermochromic response of the SP is interesting in its own right as a way to map the localized heating during dynamic fracture when combined with a microscale fluorescence mapping technique.

EXPERIMENTAL

To examine the high strain-rate response of mechanochromic and thermochromic PMMA we first synthesized samples of SP molecules incorporated in a crosslinking configuration into a PMMA matrix. A modified procedure previously reported by Moore and coworkers was used for the synthesis of the SP;⁸ the Supporting Information contains full synthesis details. We synthesized PMMA disks in a manner similar to that reported by Kingsbury et al.¹⁶ using the following method: methyl methacrylate monomer, benzoyl peroxide initiator, ethylene glycol dimethacrylate (EGDMA) crosslinker, dimethyl aniline, and acrylate-functionalized SP were added to a glass vial. The vial was then sparged with nitrogen, sealed with electrical tape, and allowed to stand in a room temperature water bath overnight to mitigate hot

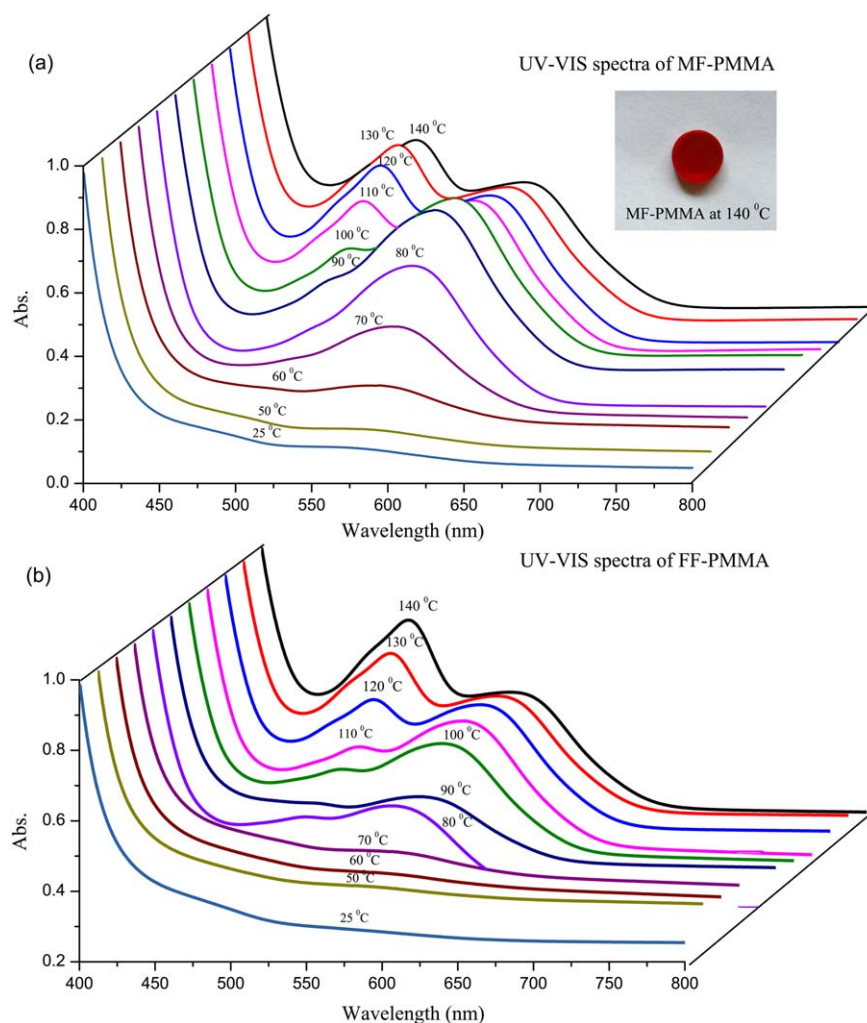


FIGURE 2 Temperature-dependent UV-vis spectra of (a) monofunctional and (b) difunctional SP-PMMA. Both systems begin to activate thermally around 70 °C. The inset shows a fully activated MF-PMMA sample at the maximum tested temperature. [Color figure can be viewed in the online issue, which is available at wileyonlinelibrary.com.]

spot formation in the reaction. The resulting polymer was released from the vial and polished to flatness on a diamond abrasive film. Figure 1 shows the SP variants considered in this study; in addition to the standard difunctional SP mechanophore attached to the polymer at two points (DF-PMMA) [Fig. 1(a,b)], we also synthesized a monofunctional SP mechanophore that was connected to the polymer at a single point (MF-PMMA) [Fig. 1(c,d)]. This material was used as a control to help differentiate between thermal and mechanical activation. Previously Moore and coworkers demonstrated that monofunctional PMMA polymers do not activate during mechanical stretching;⁸ we confirmed the lack of activation of the MF-PMMA by testing under quasistatic loading in an Instron compressive load frame. Finally, we also synthesized a difunctional control (DC-PMMA) [Fig. 1(e,f)] as a crosslinker, comparable to the control molecule used in recent shock loading data by Grady et al.²²

High-rate compression was performed on a split Hopkinson pressure bar (SHPB); 20 mm diameter, 8' long maraging

steel bars were used, with a 12" striker bar fired from a nitrogen-driven gas gun and a small copper pulse shaper to minimize wave dispersion and ensure a constant strain-rate event. With this striker, the entire compressive loading wave is applied and released on the PMMA samples within a 100 μ s timeframe. A schematic of the SHPB setup is shown in Figure 3(c). Stress and strain on the sample were analyzed with standard 350 ohm strain gauges fed into a signal amplifier, and all samples/fragments were recovered via a small collection apparatus around the impact point. A stress-reversal technique employing a momentum trap was used on the SHPB so that only a single compressive loading event occurred on the sample. All testing was performed with minimal ambient light to minimize reversion.

RESULTS AND DISCUSSION

Visible activation of the SP was observed in all cases in both the DF and MF samples following high-rate compressive loading. However, the nature of the activation (thermal

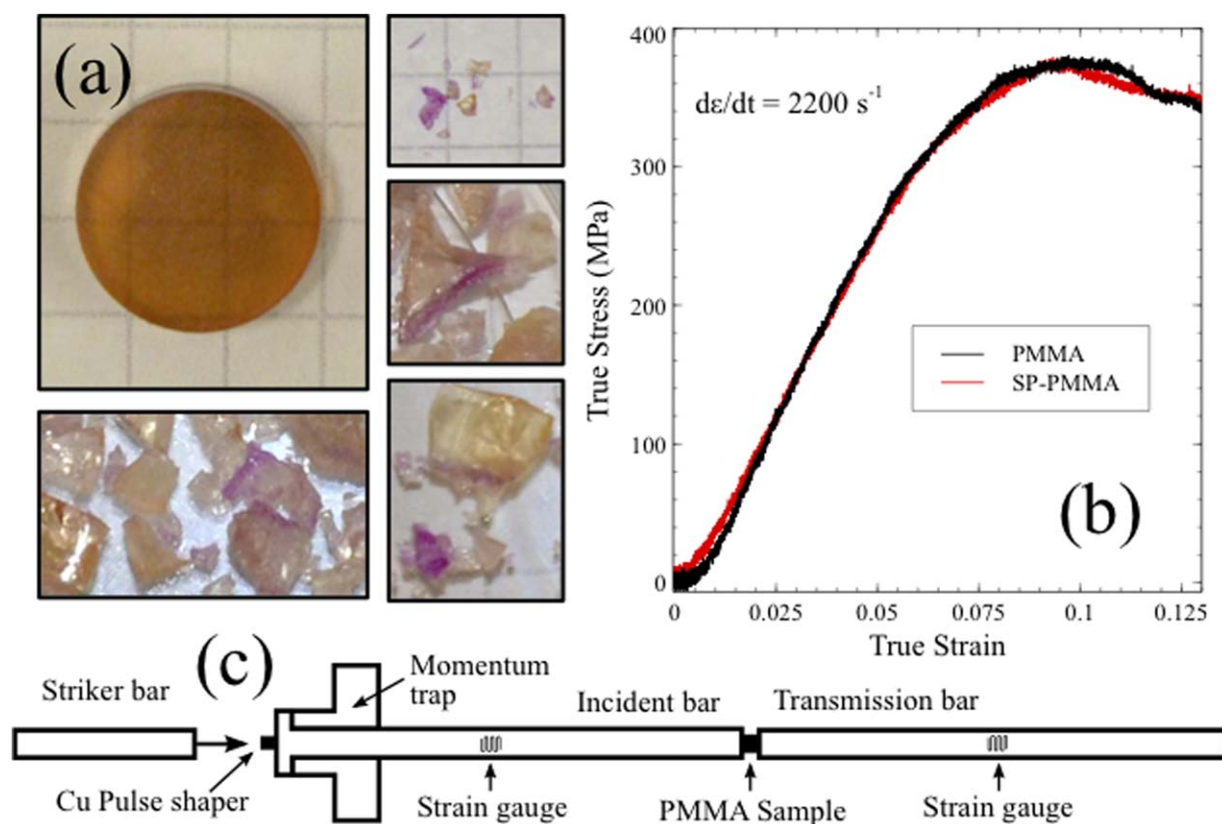


FIGURE 3 (a) Crosslinked SP-PMMA before and after high-rate impact. Recovered fragments show activation particularly around fracture surfaces. (b) Dynamic stress/strain of SP-doped and pure PMMA, showing no effect on mechanical properties from the sensor. (c) The split Hopkinson pressure bar configuration used for all mechanical impact experiments. [Color figure can be viewed in the online issue, which is available at wileyonlinelibrary.com.]

versus mechanical) is complicated by the localized temperature increases that accompany high-rate deformation in glassy polymers. As discussed above, relatively modest temperatures (around 50 °C in PMA)⁸ can activate the DF and MF SP to their colored forms, depending on the polymer matrix; previous literature suggests these temperatures are likely to be achieved in the plastic dissipation zone of a high-rate crack in PMMA.^{23–25} Thus, we first study the thermal dependence of the SP to MC conversion in all samples before interpreting the high-rate activation.

In Figure 2, we present the temperature-dependent UV-vis spectra for MF- and DF-PMMA systems. Spectra were measured using an Agilent Technologies Cary 5000 UV-vis-NIR spectrophotometer with its UV-vis source in the double beam mode. Data was collected on thin uniform disks from 400 to 800 nm using one accumulation with a one second collection time. Neither source or detector changeover was required for this wavelength range. Data are normalized based on the absorption at 400 nm, and additional two-dimensional plots of the UV-vis spectra can be found in Figure S1 in the Supporting Information. The difunctional control DC-PMMA was found to be inert under heating, activating only under UV irradiation. In both MF and DF samples, the characteristic absorption for the merocyanine at

575 nm begins to become prominent around 70 °C. An additional peak around 496 nm begins to appear at roughly 70 °C and becomes prominent above 100 °C. This feature is likely related to thermal decomposition of the MC form, and is not observed during heating of a neat PMMA sample that is crosslinked only with EGDMA. Unlike the SP absorption, this new feature does not disappear when samples are exposed to visible light. Thus, overall the thermal response of the MF and DF forms are similar, but the former is inactive under mechanical loading provided that any temperature increases due to the loading are negligible. To ensure consistency with previous reports, we also synthesized SP in linear PMA and PMMA, and confirmed that the former activates above ~50 °C and the latter is thermally inactive up to 140 °C. The synthesis of these followed the procedure by Davis et al.⁸

We next consider our impact tests. At high strain-rates ($>10^3 \text{ s}^{-1}$), our PMMA samples shattered during loading, and activation was primarily observed around fracture surfaces. A range of loading rates in this regime was attempted with different samples, and all showed qualitatively similar behavior. Figure 3(a) shows a typical PMMA sample pre-shot (12.7 mm diameter, 5.8 mm length) as well as a sample of fragments of DF and MF collected immediately following

various impact events. The activation is highly heterogeneous. In all cases small, heavily colored fragments were recovered and significant sensor activation was observed at the edges of many large fragments. Widespread uniform conversion to MC was not observed visually.

We first note that although there were significant visual changes, the small quantity of SP sensor did not alter the bulk dynamic response of the polymer. Figure 3(b) shows controlled SHPB stress/strain curves for neat PMMA and SP-PMMA including the sensor molecule. For these tests the SP-PMMA and neat PMMA were machined and polished to identical sizes, and the constant strain-rate region of the loading pulse was the same within $\sim 2\%$. The dynamic stress/strain response was nearly identical at these high-rate conditions. This similar mechanical response reflects what was observed at lower strain-rates;²¹ the small quantity of SP present did not measurably affect the bulk mechanics of the polymer. We note that the neat PMMA was synthesized using EGDMA to maintain a similar crosslinking density as the SP-PMMA samples. The MF-PMMA was sensitive to thermal activation, but did not activate under strain or compressive failure during quasistatic compression in an Instron load frame, consistent with previous work.²¹

At the macroscale, similar activation was observed in both the MF and DF PMMA, suggesting that the majority of activation is likely thermal in origin. However, further microscale analysis of the fluorescence on fracture surfaces revealed that while thermal activation appears to be dominant, some systematic differences exist between the two SP configurations. The fluorescent emission at recovered fragment surfaces was quantified in the following way. All samples were analyzed using an inVia confocal Raman microspectrometer equipped with an optical microscope. This technique provides a very high degree of spatial resolution ($\sim 1\ \mu\text{m}$) to analyze the sensor activation near microstructural features. A 514 nm Ar ion laser was used to excite the sample at a power density of $\sim 230\ \text{W}/\text{cm}^2$. Fluorescence emission was collected between 590 and 680 nm to capture the broad emission band of the merocyanine molecule, which was found to be centered at $\sim 625\ \text{nm}$. Figure 4 shows microscale intensity maps of dynamic fracture surfaces following Hopkinson bar compression, given as number of counts at 625 nm. Measurements were generally taken within eight hours of impact, and kept in a dark enclosure except during the fluorescent mapping process. We note that despite the low laser power used there is still a small effect from the 514 nm laser on the degree of activation; we have compensated for this effect in all maps presented here. Further details on this mapping technique are discussed in a separate work.²⁶ If kept in the dark, however, samples can be measured with repeatable results for multiple days beyond the impact event.

It is challenging to quantify the absolute fluorescent emission intensity, because it varies with surface roughness, collection optics, and sample thickness. For all presented

figures, we have chosen flat fracture surfaces and taken background scans of fluorescence before and after impact to ensure that we are seeing distinct activation above background and that our relative intensity changes are meaningful. The bottom left frame of Figure 4 shows the natural state of MF-PMMA, where the intrinsic noise level of the sample due to roughness and other effects is ~ 50 counts. Following impact, activation four to five times this level is observed at fracture surfaces. We note that due to the confocal nature of the Raman spectrometer the collection volume extends a small depth into the sample.

All observed high-rate fracture surfaces in both the MF and DF SP-PMMA show large increases in the 625 nm emission fluorescence, corresponding to SP activation. The first and second rows in Figure 2 show representative optical images and fluorescence intensity maps, respectively, of typical fracture surfaces. The DF-PMMA shows additional activation at certain microscale features; this is discussed in more detail below. However, on the vast majority of fracture surfaces we observe a broad, featureless activation well above the background in both the MF and DF. As shown in the top frames of Figure 4, following high-rate loading we observed the scallop pattern on the crack surface seen in many previous reports and likely arising from secondary microcracks that intersect the primary crack tip and create small level differences.^{27,28} The broad activation on these fracture surfaces was generally uniform and did not follow the features of the conic patterns. Quasistatic fracture surfaces of each material were also examined by making a small notch on the edge of PMMA disks and manually striking the sample adjacent to the notch. No activation above background was observed following this manner of low-rate fracture.

The similarities in difunctional and monofunctional forms, combined with the lack of any fluorescent intensity change under quasistatic loading, indicates this broad activation is likely caused by rapid heat dissipation due to fast-running cracks during glassy fracture of PMMA. Previous work by Bjerke and Lambros reported temperature increases of 20–70 K near cracks in PMMA during high strain-rate loading; their *in situ* measurements used a high speed infrared detector array and focusing optics.^{23,24} These temperatures are consistent with those necessary to thermally activate the SP, and while we cannot place an upper bound on the temperature with the current SP sensor molecule, this suggests that the basic monofunctional SP can provide useful microscale thermal information postmortem without the use of high-speed equipment.

One consistent difference between MF and DF forms was observed across a range of fragments. In the difunctional sample (labeled DF-PMMA in Fig. 4), we observe additional strong activation beyond this broad thermal effect in close proximity to certain microstructural features. These appear as a strong fluorescent intensity primarily within and directly adjacent to crack channels, particularly in small craze-like regions that intersect with the fracture surfaces.

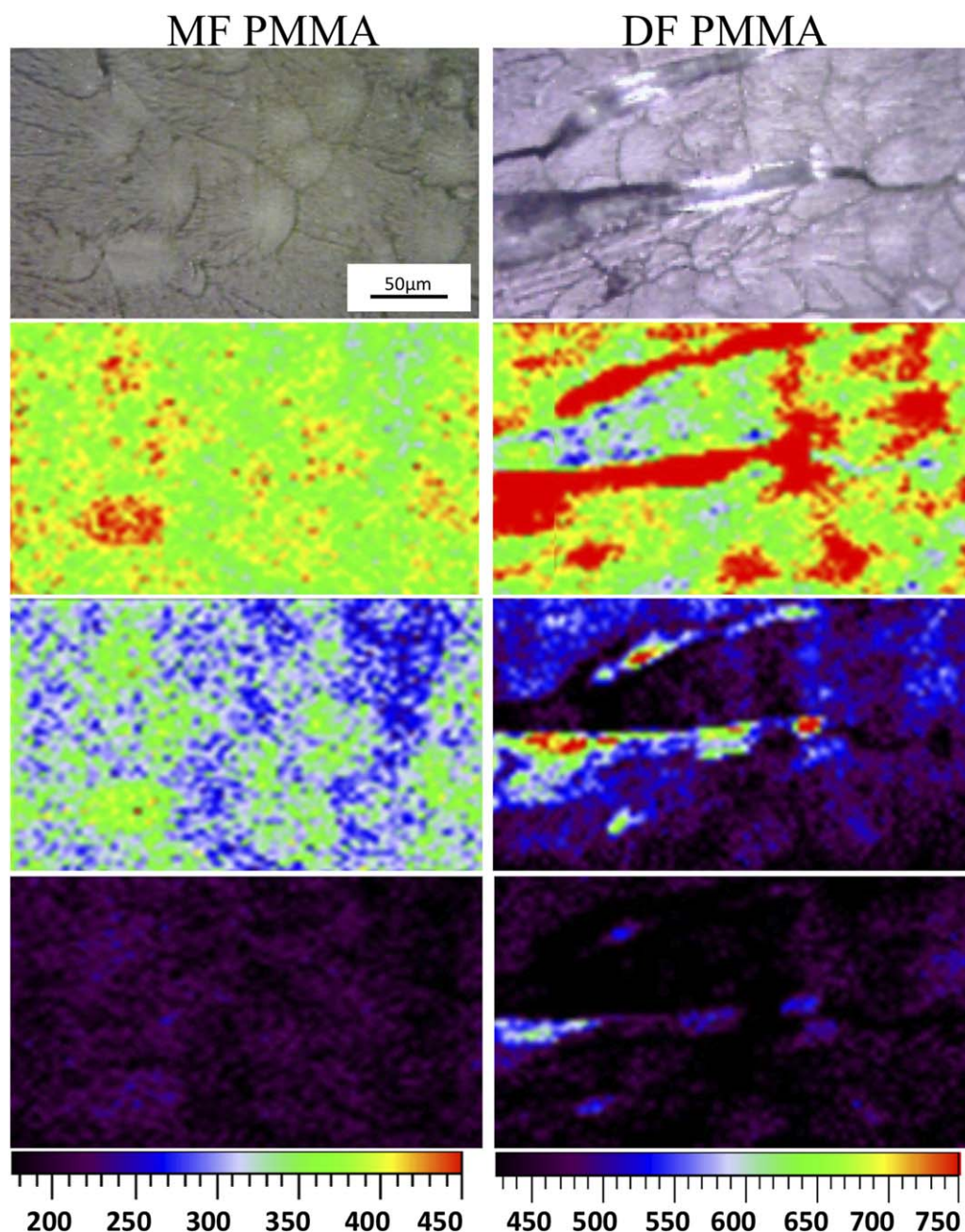


FIGURE 4 Postmortem fluorescent intensity of exposed dynamic crack surfaces. The left column shows monofunctional SP-PMMA and the right column shows the difunctional form. The scale is identical in all pictures. The second row shows fluorescent activity immediately following impact, and the final two rows show activity after 12 and 24 h of direct light exposure, respectively. [Color figure can be viewed in the online issue, which is available at wileyonlinelibrary.com.]

These are small features and do not constitute the majority of the SP activation. The right column of Figure 4 shows a representative image of this effect in difunctional SP-PMMA. Inside a craze region, PMMA fibrils temporarily bridge a small opening that is geometrically similar to a thin crack. As the craze continues to open, these fibrils thicken and are eventually pulled into tension and rupture. Many details of how crazing and fibril rupture change under very rapid loading are still controversial. Plastic heating likely occurs during

this process, but the extent of the plastic work dissipated as heat in the craze zone is unclear.²⁵ We observe no similar features in the monofunctional PMMA; a similar craze-like region showing no activation in the MF-PMMA is given in Figure 5. This suggests that local tensile forces during fibril rupture in craze zones or residual strain within the region may be responsible for the additional SP activation near crack tips. It is also possible that the SP crosslinking group is being damaged in these regions in a way that the

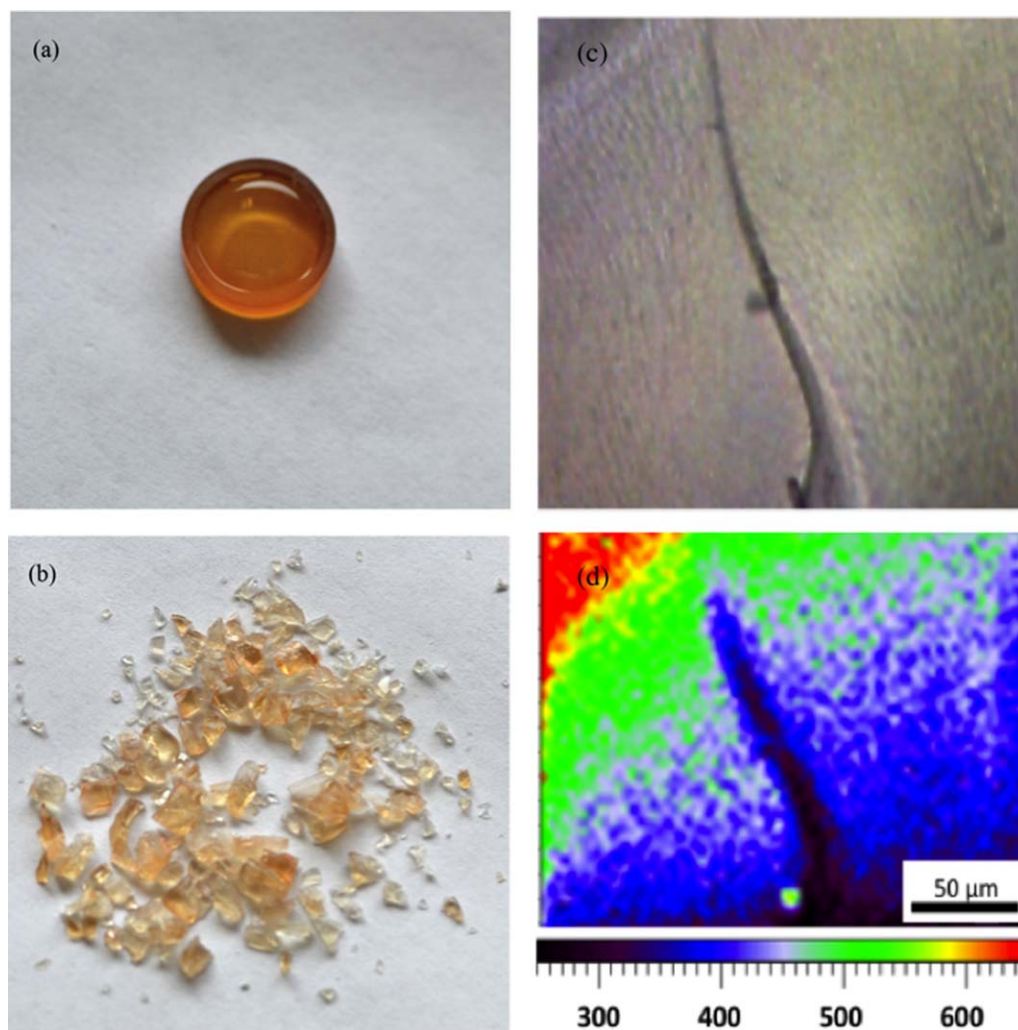


FIGURE 5 Multiple high strain-rate impacts on a difunctional DC-PMMA control sample (a) result in no SP activation in (b) recovered fragments. Frames (c) and (d) show a small craze-like feature on a crack surface of a MF-PMMA fragment following fast loading. No increased activation is observed in the feature, merely a decrease in intensity due to a change in depth. [Color figure can be viewed in the online issue, which is available at wileyonlinelibrary.com.]

MF-SP-PMMA, attached on the chains as pendants, is not. Higher magnification maps were also taken inside and around these activated zones, but additional artifacts appear in this case as height differences around the crack shift certain regions out of the focal plane of the spectrometer's optics. The maps presented here, taken with a $20\times$ optical objective, were found to be an optimal balance between resolution and repeatability.

Recent work by Degen et al. examined the rate sensitivity of this system in the opposite strain-rate regime as this study, that of quasistatic creep testing.²¹ Using full field fluorescence to determine an overall activation of the SP, they observed a power-law reduction in the activation time of the SP as a function of strain-rate between 10^{-6} and 10^{-2} s^{-1} . They concluded that considerable molecular mobility and very large deformations are necessary for mechanical activation of the SP. In contrast, recent laser shock studies by the

same group show SP activation in polystyrene at relatively modest strains (on the order of 7%) under high-rate shock loading, without large deformation of the polymer.²² In this study a difunctional control SP, similar to that shown in Figure 1(e), was used for comparison with the mechanically active difunctional mechanophore. Our results on SP cross-linked into PMMA also show considerable conversion to MC under high-rate compression at moderate strains ($<15\%$), but testing of the mechanically inert, thermally active MF-PMMA suggests that localized heating during rapid compression of the glassy polymer may be the origin of much of the activation. This heating is not prominent during standard low-rate mechanical testing, and shows the importance of accounting for thermal effects when studying the high-rate response of a mechanophore. The thermal activation of the SP is rapid in our case, occurring on the microsecond time-scale of heating processes during dynamic fracture of PMMA. No activation under heating or fast loading was observed for

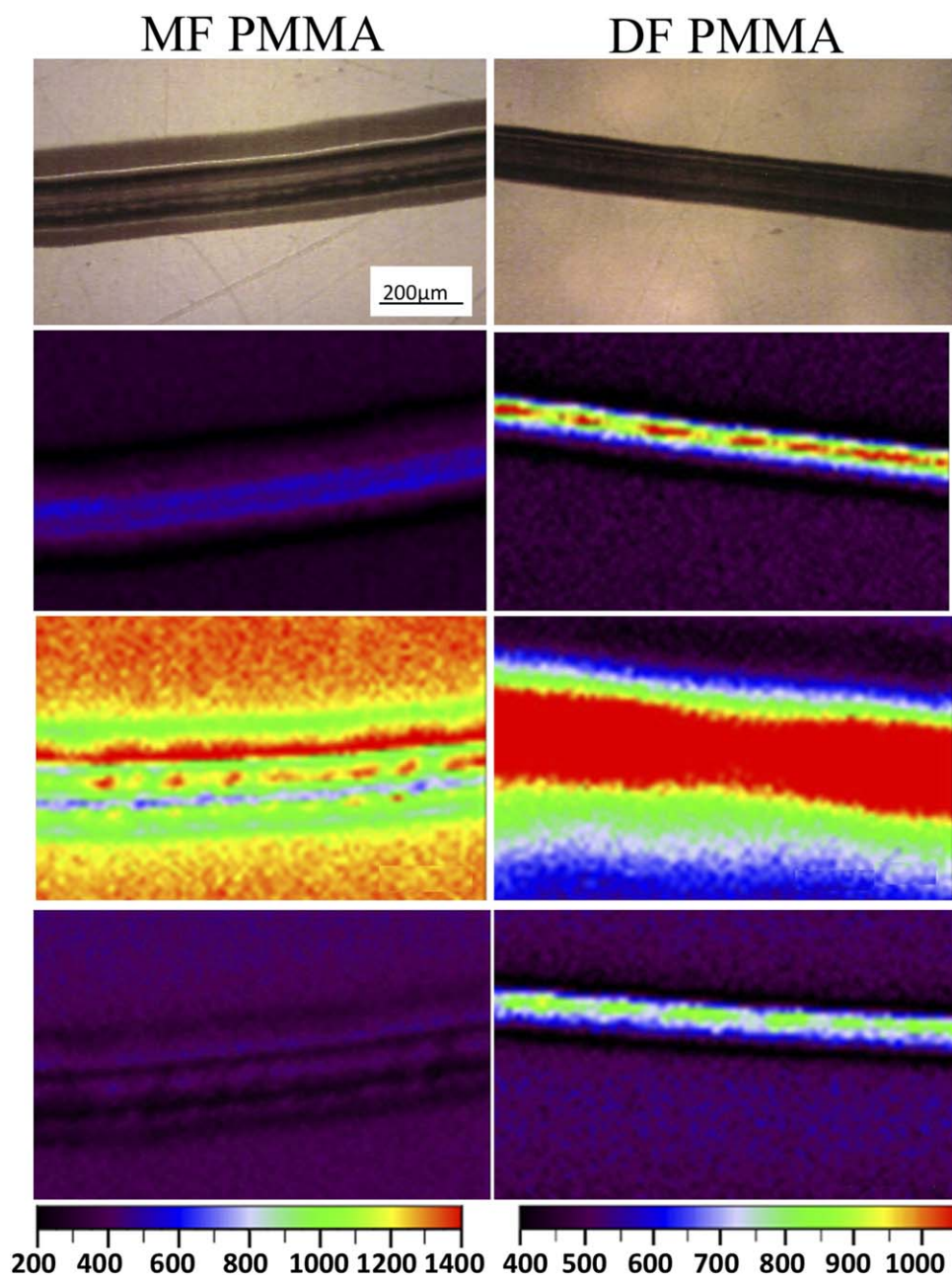


FIGURE 6 Scratch and thermal activation of monofunctional and difunctional SP-PMMA. The second row shows fluorescent activity immediately following a surface scratch, and the final two rows show activity after heating and 48 h of direct light exposure, respectively. [Color figure can be viewed in the online issue, which is available at wileyonlinelibrary.com.]

the DC-PMMA difunctional control; Figure 5(a,b) shows a sample of this material before and after repeated high-rate impacts in the Hopkinson bar with the stress-reversal momentum trap disengaged. Despite severe compression and fracture of the sample, no activation was observed visually or in any post-mortem spectrometer maps of the fragments. Recovered fragments are, however, still active when exposed to UV radiation. Widespread mechanical activation of the SP did not occur in any tested sample (DF-, MF- or DC-PMMA), even though we loaded samples well beyond the yield point and imparted considerable plastic deformation (for direct

visual comparison of the SP samples, see Fig. S2 in Supporting Information). This is not to say that no mechanochromic behavior is observed, however; we observe microscale features associated with post-yield fracture that appear to arise from in mechanical activation.

Ambient visible light slowly reconverts the SP sensor to its closed form, and in Figure 4 we present the initial fluorescence map along with maps following 12- and 24-h exposure to intense visible light (shown in the bottom two rows). Remnants of mechanical activation in the craze-like regions

can still easily be seen in fluorescent maps after many hours of light exposure. Thus while the sensor is sensitive to ambient light conditions, with the measurement technique shown here it is still possible to trace the spatial activation regions for a considerable length of time following impact. This attribute is important for pragmatic use of the SP as a means of characterizing local thermal or stressed regions. This residual activation of the difunctional form following mechanical activation is also seen on fluorescent maps following low-rate activation, discussed below.

To our knowledge, this method of microscale fluorescent mapping has not previously been used to diagnose mechanochromic polymers. To further clarify this technique and ensure it can distinguish the distinct mechanical and thermal activation, we performed additional tests on flat, non-impacted samples. Figure 6 details the progression of these tests. First, samples of both MF-PMMA and DF-PMMA were scratched with a small needle. The top row in Figure 6 shows the basic optical image of the scratch. The fluorescent image of 625 nm emission, shown in the second frame, reveals significant activation in the DF sample and minimal response in the MF, as would be expected. The third row shows identical regions following heating at 50 °C for 30 min. The heating induced widespread activation of the sensor, with major spatial variations in the fluorescent intensity here due to differences in surface heights (note the large scale bar). Finally, in the bottom row samples were exposed to direct visible light for 48 h. The MF samples showed complete reversion, while residual activation was still seen within the scratch channel in the DF sample. The origin of this residual activation is unclear, but the similarities between this simple test and the residual activation in the craze-like regions following high-rate loading lend further support to the idea that the latter is indeed mechanical in origin. The fluorescent mapping diagnostic introduced here reproduces known behavior of the SP, while also offering micron-scale resolution to identify spatial variation of this activation.

CONCLUSIONS

In conclusion, we have examined the response of a SP mechanophore at high strain-rates in solid PMMA. Additionally, we have introduced a microscale fluorescence mapping method as a diagnostic tool for mechanophore activation. The results suggest the following general high-rate behavior of the mechano- and thermochromic activation of SP when incorporated as a crosslinker in PMMA. First, the plastic heating during fast loading and fracture results in thermal activation of the SP. This is likely not a mechanochemistry response, as evidenced by similar behavior of the monofunctional form attached as a pendant to crosslinked PMMA chains. This underscores the importance of accounting for induced temperature effects during high-rate loading of mechanochromic systems. Nonetheless, the monofunctional form offers an interesting means of local temperature diagnostics when combined with a detailed fluorescent mapping.

The local temperature rise in the plastic zone of a brittle crack in glassy polymers is of great interest, and this system offers an intriguing way to study this effect without requiring fast optical diagnostics during the timescale of crack propagation.

Second, we observed evidence of some mechanical activation, particularly in regions that resemble craze zones. This occurred only in the difunctional DF-PMMA sample. In these regions, there was a very strong activation that partly remained even after multi-day exposure to direct visible light. This residual activation was also seen under in a low-rate scratch test in the confocal Raman spectrometer, even if it could not readily be seen visually at the macroscale. This provides a method for analysis of small cracks and micro-damage regions using only simple fluorescent microscopy. Finally, the fact that the sensor can respond on the fast timescales of these phenomena suggest that additional synthetic steps could be used to tune these effects and provide an intrinsic ability of glassy polymers to produce spectroscopic signals indicative of their thermal history.

ACKNOWLEDGMENTS

This work was funded by the Defense Threat Reduction Agency Basic Sciences program under grant number HDTRA139181 and managed by Su Peiris. The authors would like to thank Joel Carney, Nancy Haegel, and Markanthony Rivera for useful discussions.

REFERENCES AND NOTES

- 1 J. N. Brantley, K. M. Wiggins, C. W. Bielawski, *Polym. Int.* **2013**, *62*, 2–12.
- 2 K. M. Wiggins, J. N. Brantley, C. W. Bielawski, *ACS Macro Lett.* **2012**, *1*, 623–626.
- 3 M. M. Caruso, D. A. Davis, Q. Shen, S. A. Odom, N. R. Sottos, S. R. White, J. S. Moore, *Chem. Rev.* **2009**, *109*, 5755–5798.
- 4 J. N. Brantley, K. M. Wiggins, C. W. Bielawski, *Science* **2011**, *333*, 1606–1609.
- 5 K. M. Wiggins, J. A. Syrett, D. M. Haddleton, C. W. Bielawski, *J. Am. Chem. Soc.* **2011**, *133*, 7180–7189.
- 6 J. M. Lenhardt, A. L. Black, S. L. Craig, *J. Am. Chem. Soc.* **2009**, *131*, 10818–10819.
- 7 C. R. Hickenboth, J. S. Moore, S. R. White, N. R. Sottos, J. Baudry, S. R. Wilson, *Nature* **2007**, *446*, 423–427.
- 8 D. A. Davis, A. Hamilton, J. Yang, L. D. Cremer, D. Van Gough, S. L. Potisek, M. T. Ong, P. V. Braun, T. J. Martinez, S. R. White, J. S. Moore, N. R. Sottos, *Nature* **2009**, *459*, 68–72.
- 9 C. E. Diesendruck, B. D. Steinberg, N. Sugai, M. N. Silberstein, N. R. Sottos, S. R. White, P. V. Braun, J. S. Moore, *J. Am. Chem. Soc.* **2012**, *134*, 12446–12449.
- 10 M. B. Larsen, A. J. Boydston, *J. Am. Chem. Soc.* **2013**, *135*, 8189–8192.
- 11 A. L. Black, J. A. Orlicki, S. L. Craig, *J. Mater. Chem.* **2011**, *21*, 8460–8465.

- 12** B. A. Beiermann, S. L. B. Kramer, J. S. Moore, S. R. White, N. R. Sottos, *ACS Macro Lett.* **2012**, *1*, 163–166.
- 13** B. A. Beiermann, D. A. Davis, S. L. B. Kramer, J. S. Moore, N. R. Sottos, S. R. White, *J. Mater. Chem.* **2011**, *21*, 8443–8447.
- 14** C. K. Lee, B. A. Beiermann, M. N. Silberstein, J. Wang, J. S. Moore, N. R. Sottos, P. V. Braun, *Macromolecules* **2013**, *46*, 3746–3752.
- 15** C. K. Lee, D. A. Davis, S. R. White, J. S. Moore, N. R. Sottos, P. V. Braun, *J. Am. Chem. Soc.* **2010**, *132*, 16107–16111.
- 16** C. M. Kingsbury, P. A. May, D. A. Davis, S. R. White, J. S. Moore, N. R. Sottos, *J. Mater. Chem.* **2011**, *21*, 8381–8388.
- 17** S. Jiang, L. Zhang, T. Xie, Y. Lin, H. Zhang, Y. Xu, W. Weng, L. Dai, *ACS Macro. Lett.* **2013**, *2*, 705–709.
- 18** Y. Chen, H. Zhang, X. Fang, Y. Lin, Y. Xu, W. Weng, *ACS Macro. Lett.* **2014**, *3*, 141–145.
- 19** X. Fang, H. Zhang, Y. Chen, Y. Lin, Y. Xu, W. Weng, *Macromolecules* **2013**, *46*, 6566–6574.
- 20** G. O'Bryan, B. M. Wong, J. R. McElhanon, *ACS Appl. Mater. Interfaces* **2010**, *2*, 1594–1600.
- 21** C. M. Degen, P. A. May, J. S. Moore, S. R. White, N. R. Sottos, *Macromolecules* **2013**, *46*, 8917–8921.
- 22** M. E. Grady, B. A. Beiermann, J. S. Moore, N. R. Sottos, *ACS Appl. Mater. Int.* **2014**, *6*, 5350–5355.
- 23** T. W. Bjerke, J. J. Lambros, *Int. J. Plast.* **2002**, *18*, 549–567.
- 24** T. W. Bjerke, J. J. Lambros, *Mech. Phys. Solids* **2003**, *51*, 1147–1170.
- 25** R. Estevez, S. Basu, E. van der Giessen, *Int. J. Frac.* **2005**, *132*, 249–273.
- 26** M. van Horn, P. D. Smith, J. R. Hemmer, B. P. Mason, J. Read de Alaniz, J. P. Hooper, S. Osswald. Manuscript in preparation.
- 27** K. Ravi-Chander, J. Lu, B. Yang, Z. Zhu, *Int. J. Frac.* **2000**, *101*, 33–72.
- 28** K. Ravi-Chander, B. J. Yang, *J. Mech. Phys. Solids* **1997**, *45*, 535–563.